ACADEMIC PRESS

Available online at www.sciencedirect.com

SCIENCE DIRECT®

Journal of Sound and Vibration 264 (2003) 1139–1153

JOURNAL OF SOUND AND VIBRATION

www.elsevier.com/locate/jsvi

The dynamic analysis of a cracked Timoshenko beam by the spectral element method

M. Krawczuk[a,b], M. Palacz[b,*], W. Ostachowicz[b]

[a] *Department of Technical Sciences, University of Warmia and Mazury, Oczapowskiego 22, Olsztyn 10-736, Poland*
[b] *Institute of Fluid Flow Machinery, Polish Academy of Sciences, Fiszera 14, Gdańsk 80-231, Poland*

Received 12 March 2002; accepted 13 June 2002

Abstract

The aim of this paper is to introduce a new finite spectral element of a cracked Timoshenko beam for modal and elastic wave propagation analysis. The proposed approach deals with the spectral element method. This method is suitable for analyzing wave propagation problems as well as for calculating modal parameters of the structure. In the paper, the results of the change in modal parameters due to crack appearance are presented. The influence of the crack parameters, especially of the changing location of the crack, on the wave propagation is examined. Responses obtained at different points of the beam are presented. Proper analysis of these responses allows one to indicate the crack location in a very precise way. This fact is very promising for the future work in the damage detection field.

1. Introduction

In order to improve the safety, reliability and operational life, it is urgent to monitor the integrity of structural systems. Techniques of non-destructive damage detection in mechanical engineering structures are essential [1–3]. Previous approaches to non-destructive evaluation of structures to assess their integrity typically involved some form of human interaction. Recent advances in smart materials and structures technology has resulted in a renewed interest in developing advanced self-diagnostic capability for assessing the state of a structure without any human interaction. The goal is to reduce human interaction while at the same time monitor the

*Corresponding author. Tel.: +48-58-341-1271x109; fax: +48-58-341-6144.
E-mail addresses: mk@imp.gda.pl (M. Krawczuk), mpal@imp.gda.pl (M. Palacz), wieslaw@imp.gda.pl (W. Ostachowicz).

0022-460X/03/$ - see front matter
doi:10.1016/S0022-460X(02)01387-1

integrity of the structure. With this in mind, many researchers have made significant strides in developing damage detection methods for structures based on traditional modal analysis techniques. These techniques are often well suited for structures, which can be modelled by discrete lumped-parameter elements where the presence of damage leads to some low-frequency change in the global behaviour of the system [4–7]. On the other hand, small defects such as cracks are obscured by modal approaches since such phenomena are high-frequency effects not easily discovered by examining changes in modal mass, stiffness or damping parameters. This is because at high frequencies, modal structural models are subject to uncertainty. This uncertainty can be reduced by increasing the order of the discrete model, however, this increases the computational effort of modal-based damage detection schemes. There is also a group of methods, which utilize thermodynamic damping for assessment of the structural integrity of vibrating structures [8–10].

Spectral analysis is a method for representing the dynamic solution in the form of a series of solutions at different frequencies [11]. The spectral element method reformulates these solutions as dynamic stiffness relations, making it suitable for assembly in a manner analogous to the finite element method. A wide variety of elements have been developed for structural members over finite and semi-infinite regions. The spectral element method has several useful attributes. Since inertial properties are modelled exactly, few elements are needed to model large regions. The generalized nodes need to be placed only at structural discontinuities. Several spectral elements together can model structures having sections with different thicknesses or material properties [12]. The solution is obtained in terms of generalized displacements, subsequent calculations for velocity, acceleration, strain and stress for any applied load can then be found with relatively inexpensive post-processing calculations. The spectral element method directly computes a structure's frequency response function and in this manner gives additional information that bridges the gap between modal methods based on free vibrations and time reconstructions based on direct integration [13]. Spectral elements may also be used to solve inverse problems such as force identification. Finally, the core problem to be solved is incredibly small and is repeated many times in data-independent manner. This makes the spectral element method ideally suited for solution on computers with many processors.

At the present many spectral models of structures are available in literature. One can find spectral models of rods, beams and plates without any damage [13]. The spectral model of a cracked rod element is presented in Ref. [14]. The introduced model allows the use of propagating wave for precise localization of the crack. Spectral Bernoulli–Euler's beam with a crack is presented by Ref. [15]. The model described gives proper results for identification of crack parameters by analysis of the propagating wave. There is a model of a cracked Timoshenko beam available, but it is finite element method model [16].

This paper presents a new finite spectral Timoshenko beam element with a transverse open and non-propagating crack. This element can be applied for modal analysis and for examining the wave propagation process. Few numerical examples are presented in order to show the influence of the crack appearance on changes in modal parameters and wave propagation analysis. It is shown that the proposed element properly provides analysis of a damaged structure in order to localize and assess the size of the crack.

2. Cracked Timoshenko beam spectral element

A spectral Timoshenko beam finite element with a transverse open and non-propagating crack (crack velocity equal to zero) is presented in Fig. 1. The length of the element is L, and its area of cross-section is A. The crack is substituted by a dimensionless and massless spring, whose bending θ_b and shear θ_s flexibilities are calculated using Castigliano's theorem and laws of the fracture mechanics. This is briefly presented in the next chapter.

Nodal spectral displacements $\hat{w}$ and rotations $\hat{\phi}$ are assumed in the forms, for the left and right part of the Timoshenko beam as

$$\begin{aligned}
\hat{w}_1(x) &= R_1A_1e^{-ik_1x} + R_2B_1e^{-ik_2x} - R_1C_1e^{-ik_1(L_1-x)} - R_2D_1e^{-ik_2(L_1-x)} \quad \text{for } x\in(0,L_1),\\
\hat{\phi}_1(x) &= A_1e^{-ik_1x} + B_1e^{-ik_2x} + C_1e^{-ik_1(L_1-x)} + D_1e^{-ik_2(L_1-x)} \quad \text{for } x\in(0,L_1),\\
\hat{w}_2(x) &= R_1A_2e^{-ik_1(x+L_1)} + R_2B_2e^{-ik_2(x+L_1)} - R_1C_2E^{-ik_1[L-(L_1+x)]}\\
&\quad - R_2D_2e^{-ik_1[L-(L_1+x)]} \quad \text{for } x\in(0,L-L_1),\\
\hat{\phi}_2(x) &= A_2e^{-ik_1(x+L_1)} + B_2e^{-ik_2(x+L_1)} + C_2e^{-ik_1[L-(L_1+x)]}\\
&\quad + D_2e^{-ik_1[L-(L_1+x)]} \quad \text{for } x\in(0,L-L_1),
\end{aligned} \tag{1}$$

where L_1 denotes the location of the crack, L is the total length of the beam, R_n is the amplitude ratios given by [13]

$$R_n = \frac{ik_nGAS_1}{(GAS_1k_n^2 - \rho A\omega^2)}, \quad n = 1,2, \tag{2}$$

where $S_1 = ((0.87 + 1.12\nu)/(1+\nu))^2$ is shear coefficient for displacement [13], ν is the Poisson ratio, G is shear modulus, ρ denotes density of the material, ω is a frequency and i is imaginary unit given as $i = \sqrt{-1}$.

The wave numbers k_1 and k_2 are the roots of the characteristic equation in the general form

$$(GAS_1EJ)k^4 - (GAS_1\rho JK_2\omega^2 + EJ\rho A\omega^2)k^2 + (\rho JS_2\omega^2 - GAS_1)\rho A\omega^2 = 0, \tag{3}$$

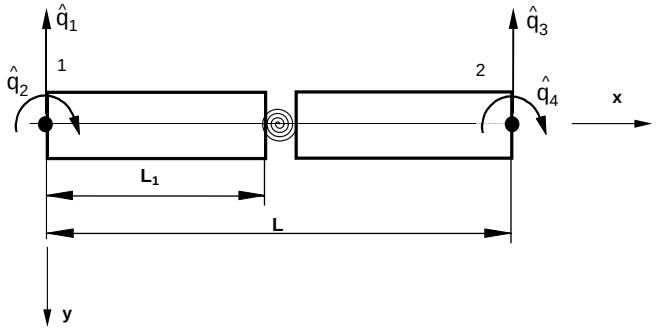

Fig. 1. The model of the Timoshenko beam with a transverse open and not propagating crack simulated by elastic hinge.

where $S_2 = 12K_1/\pi^2$ is shear coefficient for rotation [13], E denotes Young's modulus and J is second moment of area. The coefficients A_1, B_1, C_1, D_1, A_2, B_2, C_2 and D_2 can be calculated as a function of the nodal spectral displacements using the boundary conditions:

At the left end of the element

$$\hat{w}_1(x=0) = \hat{q}_1, \qquad \hat{\phi}_1(x=0) = \hat{q}_2. \tag{4}$$

At the crack location (total change of displacements and rotation angle, compatibility of bending moments and shear forces)

$$\begin{aligned}
&\hat{w}_2(x=0) - \hat{w}_1(x=L_1) = \theta_s\left[\frac{\partial \hat{w}_1}{\partial x}(x=L_1) - \hat{\phi}_1(x=L_1)\right],\\
&\hat{\phi}_2(x=0) - \hat{\phi}_1(x=L_1) = \theta_b \frac{\partial \hat{\phi}_1(x=L_1)}{\partial x},\\
&\frac{\partial \hat{\phi}_1(x=L_1)}{\partial x} = \frac{\partial \hat{\phi}_2(x=0)}{\partial x}, \quad \frac{\partial \hat{w}_1(x=L_1)}{\partial x} - \hat{\phi}_1(x=L_1) = \frac{\partial \hat{w}_2(x=0)}{\partial x} - \hat{\phi}_2(x=0).
\end{aligned} \tag{5}$$

At the right end of the element

$$\hat{w}_2(x=L-L_1) = \hat{q}_3, \qquad \hat{\phi}_2(x=L-L_1) = \hat{q}_4. \tag{6}$$

By considering the formulae describing the nodal spectral displacements for the left and right part of the Timoshenko beam, the boundary conditions can be written in a matrix form as

$$\begin{bmatrix}
R_1 & R_2 & -R_1p_1 & -R_2p_2 & 0 & 0 & 0 & 0\\
1 & 1 & p_1 & p_2 & 0 & 0 & 0 & 0\\
p_1[R_1+\theta_s(-\mathrm{i}R_1k_1-1)] & p_2(R_2+\theta_s(-\mathrm{i}R_2k_2+1) & \theta_s(-\mathrm{i}R_1k_1-1)-R_1 & \theta_s(-\mathrm{i}R_2k_2-1)-R_2 & -R_1p_1 & -R_2p_2 & R_1p_3 & R_2p_4\\
p_1(1-\mathrm{i}k_1\theta_b) & p_2(1-\mathrm{i}k_2\theta_b) & 1+\mathrm{i}k_1\theta_b & 1+\mathrm{i}k_2\theta_b & -p_1 & -p_2 & -p_3 & -p_4\\
-p_1\mathrm{i}k_1 & -p_2\mathrm{i}k_2 & \mathrm{i}k_1 & \mathrm{i}k_2 & p_1\mathrm{i}k_1 & p_2\mathrm{i}k_2 & -p_3\mathrm{i}k_1 & -p_4\mathrm{i}k_2\\
p_1(-1-\mathrm{i}R_1k_1) & p_2(-1-\mathrm{i}R_2k_2) & -1-\mathrm{i}R_1k_1 & -1-\mathrm{i}R_2k_2 & p_1(1+\mathrm{i}R_1k_1) & p_2(1+\mathrm{i}R_2k_2) & p_3(1+\mathrm{i}R_1k_1) & p_4(1+\mathrm{i}R_2k_2)\\
0 & 0 & 0 & 0 & R_1p_5 & R_2p_6 & -R_1 & -R_2\\
0 & 0 & 0 & 0 & p_5 & p_6 & 1 & 1
\end{bmatrix}
\times
\begin{bmatrix} A_1\\ B_1\\ C_1\\ D_1\\ A_2\\ B_2\\ C_2\\ D_2 \end{bmatrix}
=
\begin{bmatrix} \hat{q}_1\\ \hat{q}_2\\ 0\\ 0\\ 0\\ 0\\ \hat{q}_3\\ \hat{q}_4 \end{bmatrix}, \tag{7}$$

where

$$\begin{aligned}
&p_1 = \exp(-\mathrm{i}k_1L_1), \qquad p_2 = \exp(-\mathrm{i}k_2L_1), \qquad p_3 = \exp[-\mathrm{i}k_1(L-L_1)],\\
&p_4 = \exp[-\mathrm{i}k_2(L-L_1)], \qquad p_5 = \exp(-\mathrm{i}k_1L), \qquad p_6 = \exp(-\mathrm{i}k_2L),
\end{aligned} \tag{8}$$

The formulae below relate the coefficients A_1, B_1, C_1, D_1, A_2, B_2, C_2 and D_2 to the nodal spectral displacements by

$$\begin{aligned}
A_1 &= D_{11}^{-1}\hat{q}_1 + D_{12}^{-1}\hat{q}_2 + D_{17}^{-1}\hat{q}_3 + D_{18}^{-1}\hat{q}_4, \quad B_1 = D_{21}^{-1}\hat{q}_1 + D_{22}^{-1}\hat{q}_2 + D_{27}^{-1}\hat{q}_3 + D_{28}^{-1}\hat{q}_4,\\
C_1 &= D_{31}^{-1}\hat{q}_1 + D_{32}^{-1}\hat{q}_2 + D_{37}^{-1}\hat{q}_3 + D_{38}^{-1}\hat{q}_4, \quad D_1 = D_{41}^{-1}\hat{q}_1 + D_{42}^{-1}\hat{q}_2 + D_{47}^{-1}\hat{q}_3 + D_{48}^{-1}\hat{q}_4,\\
A_2 &= D_{51}^{-1}\hat{q}_1 + D_{52}^{-1}\hat{q}_2 + D_{57}^{-1}\hat{q}_3 + D_{58}^{-1}\hat{q}_4 \quad B_2 = D_{61}^{-1}\hat{q}_1 + D_{62}^{-1}\hat{q}_2 + D_{67}^{-1}\hat{q}_3 + D_{68}^{-1}\hat{q}_4,\\
C_2 &= D_{71}^{-1}\hat{q}_1 + D_{72}^{-1}\hat{q}_2 + D_{77}^{-1}\hat{q}_3 + D_{78}^{-1}\hat{q}_4 \quad D_2 = D_{81}^{-1}\hat{q}_1 + D_{82}^{-1}\hat{q}_2 + D_{87}^{-1}\hat{q}_3 + D_{88}^{-1}\hat{q}_4,
\end{aligned} \tag{9}$$

where D_{ij}^{-1} denotes the elements of the inverse matrix of the matrix from Eq. (7).

The nodal spectral forces ($\hat{T}$ the shear force, $\hat{M}$ the bending moment) can be determined by differentiating the spectral displacements with respect to x, and then can be expressed in the matrix form as

$$\begin{bmatrix} \hat{T}_1 \\ \hat{M}_1 \\ \hat{T}_2 \\ \hat{M}_2 \end{bmatrix} = \begin{bmatrix} r_1 & r_2 & p_1 r_1 & p_2 r_2 & 0 & 0 & 0 & 0 \\ \mathrm{i}EJk_1 & \mathrm{i}EJk_2 & -p_1\mathrm{i}EJk_1 & -p_2\mathrm{i}EJk_2 & 0 & 0 & 0 & 0 \\ 0 & 0 & 0 & 0 & -p_5 r_1 & -p_6 r_2 & -r_1 & -r_2 \\ 0 & 0 & 0 & 0 & -p_5\mathrm{i}EJk_1 & -p_6 EJk_2 & \mathrm{i}EJk_1 & \mathrm{i}EJk_2 \end{bmatrix} \times \begin{bmatrix} A_1 \\ B_1 \\ C_1 \\ D_1 \\ A_2 \\ B_2 \\ C_2 \\ D_2 \end{bmatrix}, \tag{10}$$

where $r_1 = -EJk_1^2 + \rho J\omega^2, \quad r_2 = -EJk_2^2 + \rho J\omega^2$.

From relations (9) and (10), the square matrix (4×4), which denotes the frequency-dependent dynamic stiffness for the Timoshenko beam spectral element with transverse open and non-propagating crack, can be calculated.

As the length of the spectral Timoshenko beam finite element can be very large, the computation of responses between nodes is necessary. Displacements at any point of the Timoshenko beam element can be calculated from the relationships

for $0 \leqslant x \leqslant L_1$

$$\begin{aligned}
\hat{w}(x) = {} & R_1(D_{11}^{-1}\hat{q}_1 + D_{12}^{-1}\hat{q}_2 + D_{17}^{-1}\hat{q}_3 + D_{18}^{-1}\hat{q}_4)\mathrm{e}^{-\mathrm{i}k_1 x}\\
& + R_2(D_{21}^{-1}\hat{q}_1 + D_{22}^{-1}\hat{q}_2 + D_{27}^{-1}\hat{q}_3 + D_{28}^{-1}\hat{q}_4)\mathrm{e}^{-\mathrm{i}k_2 x}\\
& - R_1(D_{31}^{-1}\hat{q}_1 + D_{32}^{-1}\hat{q}_2 + D_{37}^{-1}\hat{q}_3 + D_{38}^{-1}\hat{q}_4)\mathrm{e}^{-\mathrm{i}k_1(L_1 - x)}\\
& - R_2(D_{41}^{-1}\hat{q}_1 + D_{42}^{-1}\hat{q}_2 + D_{47}^{-1}\hat{q}_3 + D_{48}^{-1}\hat{q}_4)\mathrm{e}^{-\mathrm{i}k_1(L_1 - x)},
\end{aligned}$$

for $L_1 < x \leqslant L_2$

$$\begin{aligned}\hat{w}(x) = {} & R_1(D_{51}^{-1}\hat{q}_1 + D_{52}^{-1}\hat{q}_2 + D_{57}^{-1}\hat{q}_3 + D_{58}^{-1}\hat{q}_4)\mathrm{e}^{-\mathrm{i}k_1(L_1+x)} \\ & + R_2(D_{61}^{-1}\hat{q}_1 + D_{62}^{-1}\hat{q}_2 + D_{67}^{-1}\hat{q}_3 + D_{68}^{-1}\hat{q}_4)\mathrm{e}^{-\mathrm{i}k_2(L_1+x)} \\ & - R_1(D_{71}^{-1}\hat{q}_1 + D_{72}^{-1}\hat{q}_2 + D_{77}^{-1}\hat{q}_3 + D_{78}^{-1}\hat{q}_4)\mathrm{e}^{-\mathrm{i}k_1[L-(x+L_1)]} \\ & - R_2(D_{81}^{-1}\hat{q}_1 + D_{82}^{-1}\hat{q}_2 + D. \end{aligned} \tag{11}$$

3. Flexibilities at the crack location

Coefficients of the beam flexibility matrix at the crack location (in general form) can be calculated using the Castigliano theorem [17]

$$c_{ij} = \frac{\partial^2 U}{\partial S_i \partial S_j} \quad \text{for } i = 1, \ldots, 6, \quad j = 1, \ldots, 6, \tag{12}$$

where U denotes the elastic strain energy of the element caused by the presence of the crack and are the independent nodal forces acting on the element.

For the analyzed beam, the elastic strain energy due to the crack appearance [18] can be expressed by

$$U = \frac{1}{E}\int_A (K_{\mathrm{I}}^2 + K_{\mathrm{II}}^2)\,\mathrm{d}A, \tag{13}$$

where A denotes the area of the crack, K_{I} and K_{II} are a stress intensity factors corresponding to the first and second mode of the crack growth [19].

The stress intensity factors can be calculated as

$$K_{\mathrm{I}} = \frac{6M}{BH^2}\sqrt{\pi\alpha}F_{\mathrm{I}}\left(\frac{\alpha}{H}\right), \qquad K_{\mathrm{II}} = \frac{\beta T}{BH}\sqrt{\pi\alpha}F_{\mathrm{II}}\left(\frac{\alpha}{H}\right), \tag{14}$$

where M is a bending moment, β denotes shear factor [20], T is a shear force, B, H, α are dimensions—see Fig. 2, F_{I} and F_{II} are a correction function in the form [19]

$$\begin{aligned} F_{\mathrm{I}}\left(\frac{\alpha}{H}\right) &= \sqrt{\frac{\tan(\pi\alpha/2H)}{\pi\alpha/2H}}\,\frac{0.752 + 2.02(\alpha/H) + 0.37[1-\sin(\pi\alpha/2H)]^3}{\cos(\pi\alpha/2H)}, \\ F_{\mathrm{II}}\left(\frac{\alpha}{H}\right) &= \frac{1.30 - 0.65(\alpha/H) + 0.37(\alpha/H)^2 + 0.28(\alpha/H)^3}{\sqrt{1-(\alpha/H)}}. \end{aligned} \tag{15}$$

After simple transformations, the modelling of the flexibilities of the elastic elements cracked cross-section of the Timoshenko beam spectral finite element, can be rewritten as

$$c_b = \frac{72\pi}{BH^2}\int_0^{\bar{a}} \bar{\alpha}F_{\mathrm{I}}^2(\bar{\alpha})\,\mathrm{d}\bar{a}, \qquad c_s = \frac{2\beta\pi}{B}\int_0^{\bar{a}} \bar{\alpha}F_{\mathrm{II}}^2(\bar{\alpha})\,\mathrm{d}\bar{a}, \tag{16}$$

where $\bar{a} = a/H$, $\quad \bar{\alpha} = \alpha/H$ (see Fig. 2).

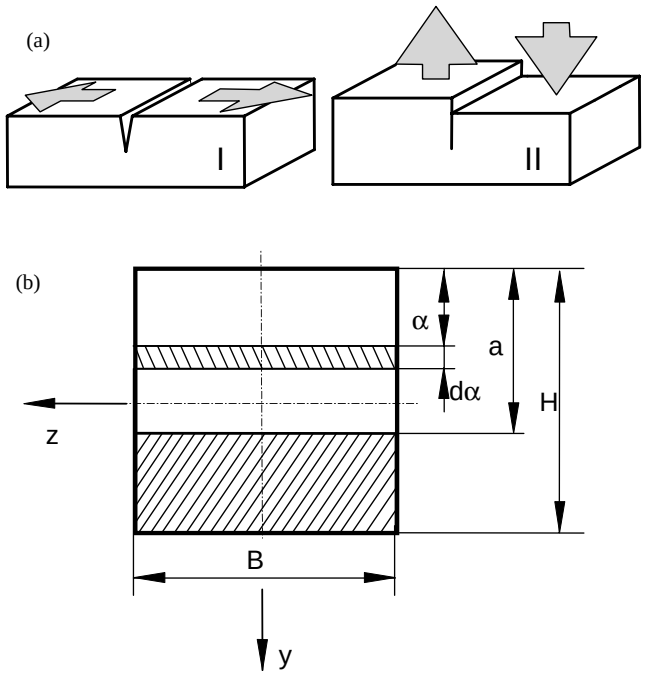

Fig. 2. (a) I and II crack propagation modes; (b) cross-section of the beam element at the crack location.

In the non-dimensional form the flexibilities can be expressed as

$$\theta_b = \frac{EJc_b}{L}, \qquad \theta_s = \frac{GAc_s}{L}. \tag{17}$$

4. Numerical examples

In the aim to demonstrate the validity of the proposed model, several numerical tests have been carried out for a cantilever beam with dimensions: length 2.0 m, height 0.02 m, width 0.02 m, Young's modulus 210 GPa, and mass density 7860 kg/m^3. In the numerical tests the model was fixed at one end and impacted at the second. The model tested consisted of two elements, one with a crack and the second the so-called throw-off element [13]. This approach allowed forward and backward moving waves to be obtained.

First and second numerical tests were done in order to show whether the proposed model is useful for modal analysis. According to the literature study and previous numerical investigations by authors using one spectral element, it is possible to analyze any range of frequencies. It is extremely important when there is a need to analyze high natural frequencies (very small defects cause detectable changes in high natural frequencies only). In such cases classical finite element models would require very dense grid, which is time consuming for computational calculations. The two examples presented show that the model allows for proper modal analysis as well as for the classical finite element one.

Table 1
Changes in first four natural frequencies (rad/s)

Relative crack depth		0.05			0.25			0.5		
Relative crack location (from the fixed end)	No crack	0.25	0.5	0.75	0.25	0.5	0.75	0.25	0.5	0.75
Finite element method model [21]										
Frequency I	26.12	26.12	26.12	26.12	25.83	25.13	25.13	25.196	25.76	25.83
Frequency II	163.72	163.72	163.72	163.72	162.15	161.94	161.55	162.09	161.71	161.67
Frequency III	457.52	457.52	457.52	457.45	456.02	455.62	455.96	454.82	455.12	449.36
Frequency IV	892.75	892.65	892.31	892.13	872.35	874.23	878.54	861.43	860.54	859.8
Frequency XVIII	Not available									
Frequency XIX	Not available									
Spectral model										
Frequency I	26.138	26.138	26.138	26.138	26.075	26.138	26.138	25.196	25.887	26.138
Frequency II	164.24	164.24	164.24	164.24	164.18	163.36	163.93	163.99	157.21	161.67
Frequency III	459.62	459.62	459.62	459.55	458.04	456.62	457.16	446.8	459.62	439.26
Frequency IV	899.75	899.69	899.63	899.63	896.30	895.23	895.54	873.43	864.5	867.9
Frequency XVIII	21459	21458	21456	21458	21441	21363	21444	21341	21258	21364
Frequency XIX	23854	23851	23854	23851	23759	23852	23763	23295	23845	23308

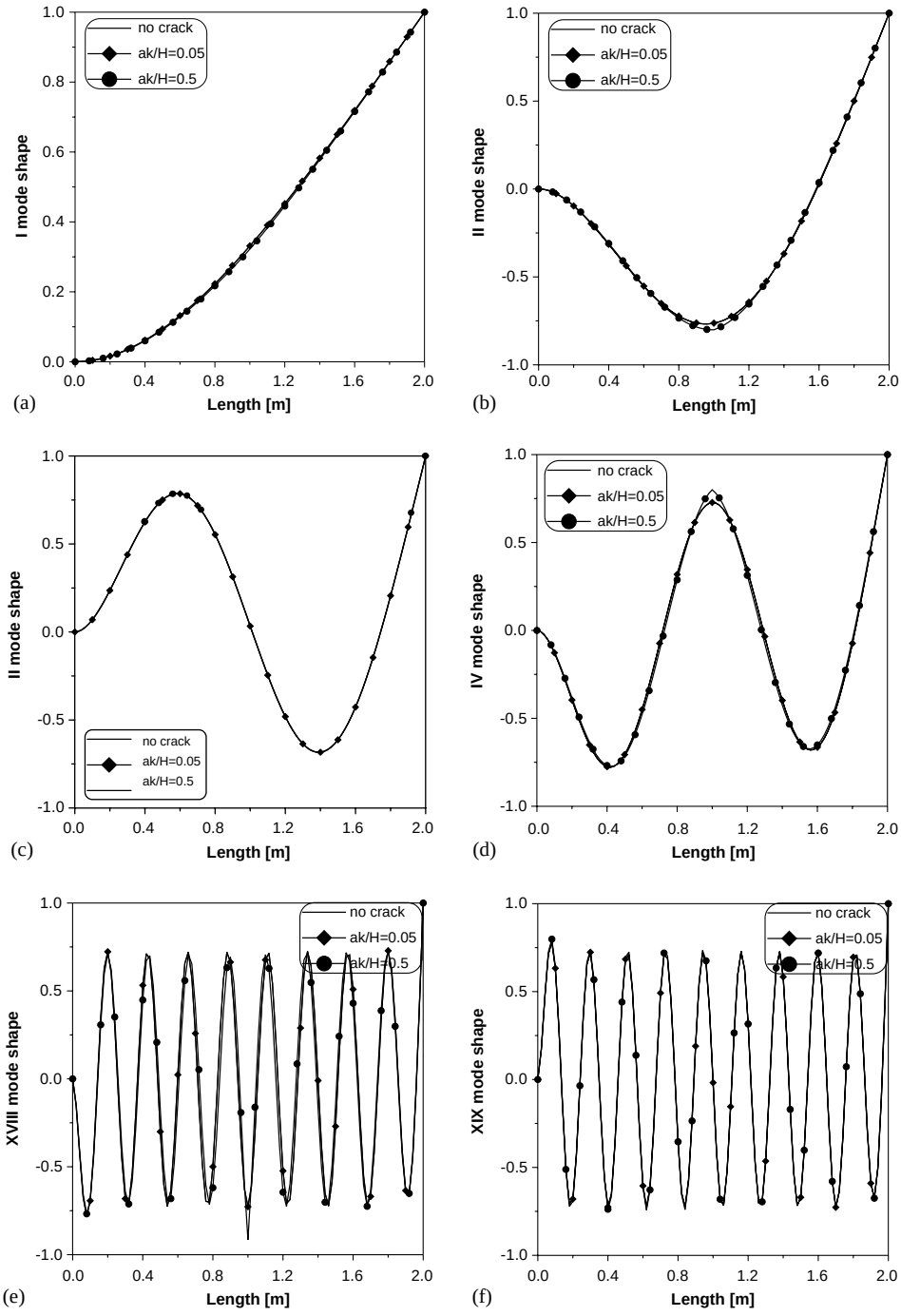

Fig. 3. Mode shapes obtained for an uncracked beam (—), for a beam with 5% of the beam height crack (—◆—) and for a beam with 50% of the beam height crack —●—: (a) I mode shape; (b) II mode shape; (c) III mode shape; (d) IV mode shape; (e) XVIII mode shape; (f) XIX mode shape.

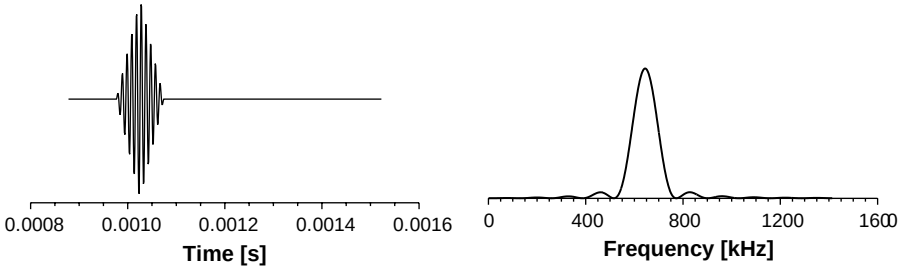

Fig. 4. Excitation triangle signal lasting for 0.0925 μs, multiplied by sinusoidal signal lasting $\frac{1}{20}$ of the duration of the triangle signal and its FFT.

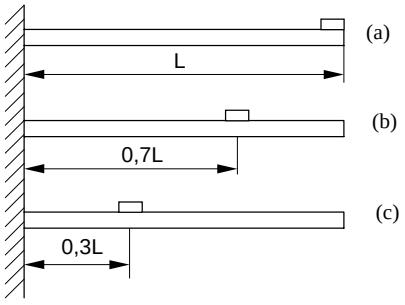

Fig. 5. Location of measured points.

In order to examine whether the localization of the crack influences the natural frequencies, a first numerical example was done. Table 1 shows the first four and two higher computed natural frequencies for a beam without a crack and for a beam with nine different crack depths and locations. For numerical calculations it was assumed that frequencies are determined with precision ± 0.005 Hz. It is noticeable that changes in natural frequencies become more intensive with the growth of the crack depth. For higher natural frequencies, even for a very small crack, changes due to crack appearance are higher than the first few ones. Results obtained for an elaborated spectral model of a Timoshenko beam were compared with results obtained for Timoshenko beam calculated from the finite element method [21]. Similar character of changes in natural frequencies for a cracked beam is reported in Ref. [22].

The next numerical example was to investigate whether the proposed model is useful for examining the changes in mode shapes due to the appearance of a crack. Fig. 3 illustrates changes in mode shapes for uncracked beams and for cracked beams with crack depths equal to 5% and 50% of the beam height precisely marked on the pictures. In both cases the crack was located in the middle of the beam. It is noticeable that the appearance of the crack leads to deformation of the calculated mode shapes.

In the numerical tests described in Ref. [14], it appeared that the kind of excitation force influences the response of a structure. For the tests described in this paper, the excitation signal is presented in Fig. 4. It is a product of a triangle signal lasting for 0.0925 μs and a sinusoid signal with the period equal to $\frac{1}{20}$ of the duration of the triangle signal. This signal produces excitation of a wide range of frequencies, thus obtaining very clear response in the time domain.

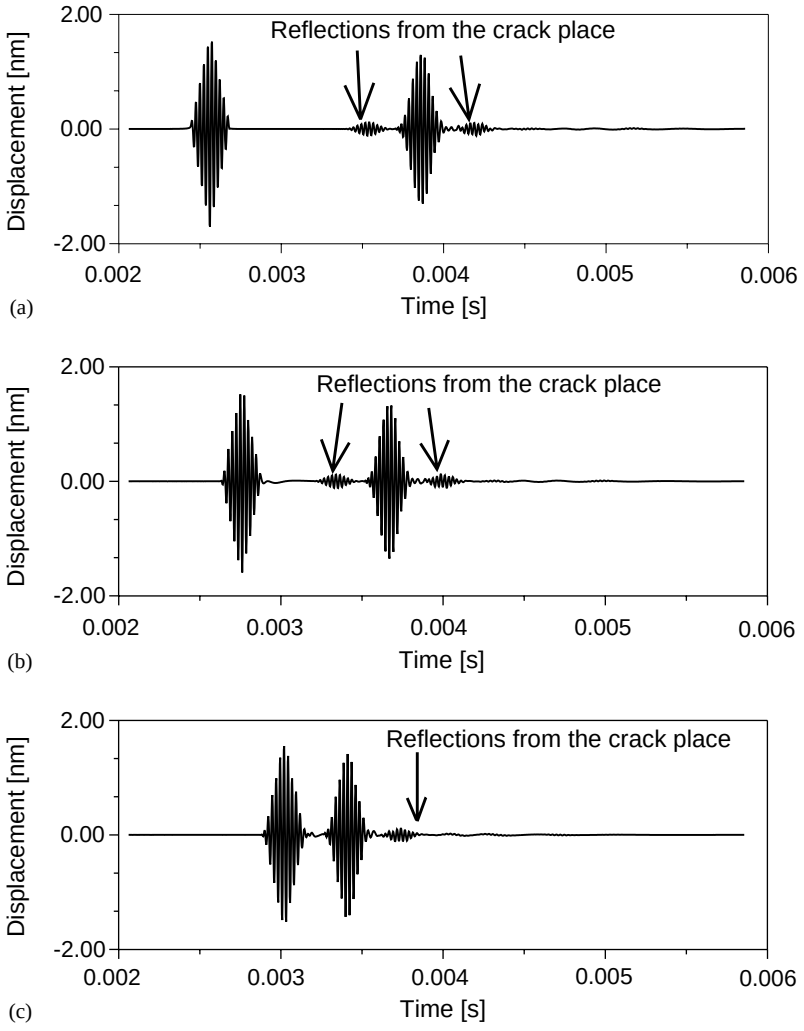

Fig. 6. Wave propagation, for a crack located at 20% of a beam height and at distance 25% of the length from the fixed end. Measurements are taken in points shown in Fig. 5.

Fig. 5 presents the location of measurement points for the next numerical examples.

The next three figures (Figs. 6–8) show the responses of the system obtained at different points of the beam for a crack of depth equal to 20% of the beam height, located at three different distances from the fixed end of the beam. Fig. 6 shows the results obtained for a crack located at a distance equal to 25% of the beam length from the fixed end. The curve in Fig. 6(a) illustrates the response measured at the impacted free node (Fig. 5(a)). It is noticeable that there are four responses on some pictures. The first response represents the excitation signal, the second the crack, the third is the reflection of the fixed end and the fourth is the second reflection from the crack location. The Fig. 6(b) presents the response of the systems shown in Fig. 5. In this case one sees again four signals, as for curve 6(a). However, for this example the excitation signal is recorded occurring later than in curve 6(a), because the wave needed to propagate from the

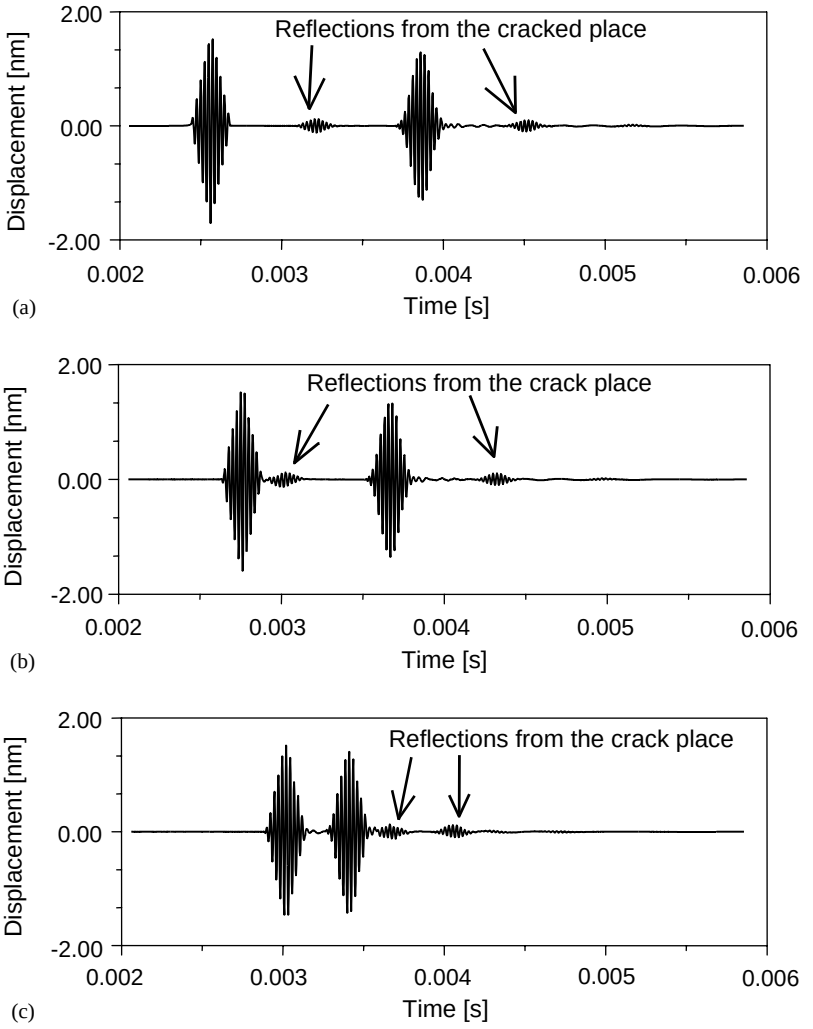

Fig. 7. Wave propagation, for a crack located at 20% of a beam height and at distance 50% of the length from the fixed end. Measurements are taken in points shown in Fig. 5.

impacted node to the point of measurement. The curve shown in Fig. 6(c) is recorded at the point shown in Fig. 5(c). One can see three signals only. First stands for the excitation signal, the second reflects the fixed end, the third is the second reflection from the crack. In this case the first reflection from the crack interfered with the second reflection from the fixed end.

Fig. 7 introduces responses of the system recorded for a crack located at the middle of the beam and is 20% of its height. Curve of Fig. 7(a) corresponds to Fig. 5(a). In this case one sees four signals. First is the excitation signal, second one is a reflection from the crack, third one is a reflection from the fixed end and fourth one is the second reflection from the crack. Fig. 7(b) shows four signals as well. The first one corresponding to Fig. 5(b) is recorded later than in Fig. 7(a) due to wave propagation from the impact point to the measurement point. Fig. 7(c) presents also four signals. Localization of recorded reflections results from with the measurement

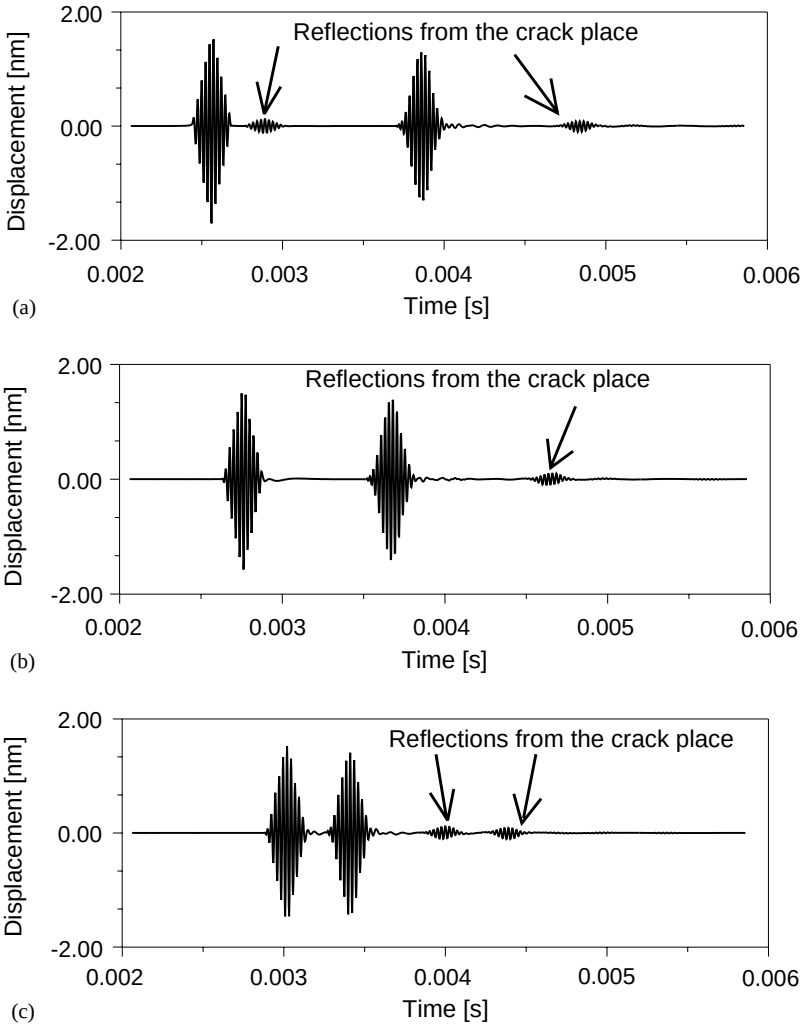

Fig. 8. Wave propagation, for a crack located at 20% of a beam height and at distance 75% of the length from the fixed end. Measurements are taken in points shown in Fig. 5.

point location (Fig. 5(c)) and the distance, which needs to be reached by the propagating wave from the impact to the point of measurement.

Fig. 8 presents results obtained for the 20% deep crack located at a distance of 75% of the beam length from the fixed end. Fig. 8(a) corresponds to the result obtained from Fig. 5(a). The first signal represents for the impact signal, the second one comes from the crack. The reflected wave propagates for a short distance from the point of measurement and the crack, which is why the first two reflections are so close to each other. The third reflection comes from the fixed end and the last one is another reflection from the crack place. The second picture (Fig. 8(b)), corresponding to Fig. 5(b) shows three reflections only. This happens from interference between the first reflection from the crack place and the reflection from the fixed end. Fig. 6(c) illustrates the response at the measurement point shown in Fig. 5(c). The first signal is the excitation signal,

adjacent is the signal reflected from the fixed end, then the first reflection from the crack place and the last is the second reflection from the crack place.

From these results one concludes that knowing the wave propagation velocity and the time of appearance of additional reflections, the location of the crack is easily calculated.

5. Conclusions

This paper has presented a new model of a Timoshenko spectral finite beam element with a transverse open and non-propagating crack. The basic difference between the classical approach and the spectral method is clearly shown. It is easily seen that the spectral approach gives more information and is more sufficient for damage detection. The elaborated element can be used not only for modal analysis, but also for wave analysis. The results obtained indicate that the current approach is capable of calculating high natural frequencies without any additional and time-consuming numerical computation.

Responses, measured at different points, from a cracked Timoshenko beam are presented. They can give information about the location of the crack and the influence of different locations of the crack on the wave propagation in the damaged structure was shown. Differences in the responses may be used for proper assessment of the crack location.

Future research work will focus on extending the spectral element method to damaged structures with more complex geometry, like for example plates or constructions built up from beam-like structures.

References

[1] Fu-Kuo Chang (Ed.), Structural Health Monitoring: Current Status and Perspectives, Technomic Publishers, Basel, 1997.
[2] Fu-Kuo Chang (Ed.), Structural Health Monitoring: Current Status and Perspectives, Technomic Publishers, Basel, 1999.
[3] M. Krawczuk, W. Ostachowicz, Damage indicators for diagnostic of fatigue cracks in structures by vibration measurements—a survey, Journal of Theoretical and Applied Mechanics 34 (2) (1996) 307–326.
[4] R.D. Adams, P. Cawley, The localisation of defects in structures from measurements of natural frequencies, Journal of Strain Analysis 14 (2) (1979) 49–57.
[5] P. Cawley, R.D. Adams, C.J. Pye, B.J. Stone, A vibration technique for non-destructively assessing the integrity of structures, Journal of Mechanical Engineering Sciences 20 (2) (1978) 93–100.
[6] A. Messina, I.A. Jones, E.J. Williams, Damage detection and localisation using natural frequency changes, Proceedings of the First Conference on Structure Identification, Cambridge, 1992, pp. 67–76.
[7] T.W. Lim, T.A.L. Kashangaki, Structural damage detection of space truss structures using best achievable eigenvectors, American Institute of Aeronautics and Astronautics Journal 30 (9) (1994) 2310–2317.
[8] S.D. Panteliou, A.D. Dimarogonas, Thermodynamic damping in materials with ellipsoidal cavities, Journal of Sound and Vibration 201 (5) (1997) 555–565.
[9] S.D. Panteliou, A.D. Dimarogonas, The damping factor as an indicator of crack severity, Theoretical and Applied Fracture Mechanics 34 (2000) 217–223.
[10] S.D. Panteliou, T.G. Chondros, V.C. Argyrakis, A.D. Dimarogonas, Damping factor as an indicator of crack severity, Journal of Sound and Vibration 241 (2) (2001) 235–245.

[11] K.A. Lakshmanan, D.J. Pines, Detecting crack size and location in composite rotorcraft flexbeams, Proceedings of the SPIE Smart Structures and Materials 3041 (1997) 408–416.
[12] K.A. Lakshmanan, D.J. Pines, Modelling damage in composite rotorcraft flexbeams using wave mechanics, Smart Materials and Structures 6 (1997) 383–392.
[13] J.F. Doyle, Wave Propagation in Structures, Springer, New York, 1997.
[14] M. Palacz, M. Krawczuk, Analysis of longitudinal wave propagation in a cracked rod by the spectral element method, Computers and Structures 80 (24) (2002) 1809–1816.
[15] M. Krawczuk, Application of spectral beam finite element with a crack and iterative search technique to damage detection, Finite Elements in Analysis and Design 38 (2002) 537–548.
[16] M. Krawczuk, Modelling and identification of cracks in truss constructions, Finite Element in Analysis and Design 16 (1992) 41–50.
[17] J.S. Przemieniecki, Theory of Matrix Structural Analysis, McGraw-Hill, New York, 1968.
[18] C.A. Papadopoulos, A.D. Dimarogonas, Coupled longitudinal and bending vibrations of a rotating shaft with an open crack, Journal of Sound and Vibration 117 (1) (1987) 81–93.
[19] H. Tada, P.C. Paris, G.R. Irwin, The Stress Analysis of Cracks Handbook, Del Research Corporation, Heller town, PA, 1973.
[20] G.R. Cowper, The shear coefficient in Timoshenko's beam theory, American Society of Mechanical Engineers, Journal of Applied Mechanics Series E 33 (2) (1966) 335–340.
[21] M. Krawczuk, Dynamics of Constructional Elements with Fatigue Cracks, Vol. 441, IFFM Publishers, gdansk, 1994, p. 1398 (in polish).
[22] P. Gudmundson, Eigenfrequency changes of structures due to cracks, notches or other geometrical changes, Journal of the Mechanics and Physics of Solids 30 (5) (1982) 339–353.